Optimization of extreme ultraviolet photons emission and collection in mass-limited laser produced plasmas for lithography application

T. Sizyuk and A. Hassanein
Center for Materials under Extreme Environment, School of Nuclear Engineering, Purdue University, West Lafayette, Indiana 47907, USA

(Received 23 March 2012; accepted 5 July 2012; published online 2 August 2012)

The progress in development of commercial system for next generation EUV lithography requires, among other factors, significant improvement in EUV photon sources such as discharge produced plasma (DPP) and laser produced plasma (LPP) devices. There are still many uncertainties in determining the optimum device since there are many parameters for the suitable and efficient energy source and target configuration and size. Complex devices with trigger lasers in DPP or with pre-pulsing in LPP provide wide area for optimization in regards to conversion efficiency (CE) and components lifetime. We considered in our analysis a promising LPP source configuration using 10–30 μm tin droplet targets, and predicted conditions for the most efficient EUV radiation output and collection as well as calculating photons source location and size. We optimized several parameters of dual-beam lasers and their relationship to target size. We used our HEIGHTS comprehensive and integrated full 3D simulation package to study and optimize LPP processes with various target sizes to maximize the CE of the system. © *2012 American Institute of Physics*. [http://dx.doi.org/10.1063/1.4740230]

I. INTRODUCTION

The history of 13.5 nm photons source development for EUV lithography includes investigation of several devices using discharge produced plasma (DPP), i.e., dense plasma focus, Z-pinch device, and hollow-cathode tube,[1] as well as devices using laser produced plasma (LPP) utilizing several target materials, i.e., xenon, lithium, and tin.[2–4] Several criteria were considered for the optimization of these systems including efficient EUV output and collection, minimized debris production and mitigation, components lifetime, and source brightness for the high volume manufacturing (HVM) devices.

Recent achievements in the development of bright EUV photon source show two distinctive directions, i.e., laser-assisted discharge plasma[5] and dual-beam laser plasma.[6] Laser beams are utilized in both cases for target vaporization and the initial creation of matter used for the subsequent ionization and plasma plume optimization for EUV devices (DPP or LPP) for maximum EUV radiation output. Parameters of the initial laser beams for creation of pre-plasma determine the temporal and spatial characteristics of EUV devices. Since several factors such as laser beam wavelength, intensity, pulse duration, spot size, target geometry, and size can significantly influence the production of radiating media with specific density and velocities, optimization of such complicated systems would require significant costly experimental efforts.

Guidance and realistic predictions of experimental results are possible with the state of the art comprehensive modeling that complies with the following important requirements: (1) computer package includes complete set of models for accurate description of all physics processes involved in LPP and DPP devices; (2) models are well tested and benchmarked separately in each interaction physics phase as well as in an integrated system; (3) simulations within the package should be able to be extended to reasonable range of experimental parameters without any parametric adjustments or fittings. Accurate modeling and comprehensive understanding of plasma physics processes in LPP should consider details of spatial and temporal input power deposition from laser sources, absorption/reflection of laser light from the surface of solid/liquid target, hydrodynamic evolution of target, absorption/reflection of laser from the evolving target vapor, atomic physics and vapor ionization, absorption/reflection in heated plasma layer, and photon generation and transport during different phases of the evolving target. HEIGHTS simulation package incorporates detail models in full 3D geometry of multiple laser interactions with various target materials for EUV lithography as well as for applications in fusion energy, nuclear and high energy physics, directed energy lethality, and surface modifications of materials.

Building on our long history in modeling EUV sources using HEIGHTS package, LLP, as well as DPP,[1,7–12] we extended our investigation of realistic LPP devices to obtain highly efficient source for maximum EUV radiation output. Our previous results showed the influence of spatial effects such as plasma geometrical confinement that depend on target geometry and can be controlled by the lasers system.[7,9] In this work, we investigated the effect of matter density in devices using small tin droplets heated by dual-pulse lasers and analyzed the behavior of mass produced from the vaporized droplet to develop an efficient mass-limited EUV source.

II. BRIEF MODELS DESCRIPTION

Key in modeling laboratory plasma devices is correct representation of target hydrodynamic evolution, plasma dynamics, various energy exchange mechanisms, and main dissipative processes. Additionally, describing laboratory

plasmas as mixture of electrons and ions is more correct and enables one to explain numerous physical phenomena, for example, in laser produced plasmas, electrons overheating and acceleration, magnetic field generation, etc., and the correct magnetohydrodynamic (MHD) equation set should be expanded to consider these additional components. The three conservation law equations should be separated (mass density, momentum, energy density) for both electron and ion parts. This approach is utilized in HEIGHTS package that has been used in numerous scientific and engineering research areas.[13–15] The package is also developed in full 3D configuration for all phases of beam/plasma-target interaction and plasma evolution processes. It combines state-of-the art models of energy deposition, vapor/plasma formation/evolution, MHD processes, thermal conduction in material and in plasma, atomic physics and resulting opacities, detailed photon radiation transport, and interaction between plasma/radiation and target material in three dimension configuration for various target designs.

Laboratory plasmas usually have high gradients of radiation energy density at small spatial lengths and require special treatment. Advanced physical/mathematical models and numerical methods should be implemented for correct interpretation of radiation energy distribution. Two main separate approaches were developed, verified, and compared in the frame of HEIGHTS simulation package for various plasma science applications: direct integration of the radiation transport equation (RTE) along photons path and Monte Carlo models with several novel weight factors to enhance the speed of calculations.[1,7]

In direct Gauss integration methods, the radiant energy flux is calculated by integrating the differential RTE along the direction of the photon transport that represents a conservation of emitted and absorbed energy. Direct Gauss integration methods digitize the MHD domain in space, energy, and angles. The radiation intensity along each direction is determined by integrating the RTE, and the directions are given by the angles of the chosen numerical quadrature.

In Monte Carlo methods, alternative to the direct solution of RTE, where one searches the continuous function of the radiation intensity, the probabilistic model of the energy redistribution operates with discrete portions of the radiative energies.[7] Accurate trajectory and number of emitted and absorbed energy portions in the plasma domain is important in energy distribution and system behavior. The energy and the trajectory of photon movement are determined by Monte-Carlo techniques. Advantage of this method is unique opportunity to determine location, size, and intensity of radiative source in any range of photons energy with accurate and flexible collection at any solid angle within the device.

Accurate description of two important processes, i.e., laser energy absorption and target material vaporization, can be critical in modeling LPP with lower laser intensities and pre-plasma creation from small targets with non-flat geometries. Ideally, the laser absorption by a target should be treated in two phases: first by the cold, unperturbed solid/liquid target and then by the target having an evolving plasma layer above the remaining solid/liquid target. This becomes important because of the complex hydrodynamic flow near the target surfaces where we should take into account the various energy inputs from laser radiation, i.e., absorption/reflection in solid/liquid target, absorption/reflection in target vapor, and absorption/reflection in plasma layer. Because, for example, the production of the initial EUV radiation area above the target surface consumes part of the laser beam energy and part of main pulse duration, the final efficiency of LPP devices increases with decreasing the time needed for such preparation stage. This entire process includes gradual decreasing of laser absorption in cold material and increasing absorption in the hot plasma. It is also important to take into account the re-absorption of laser radiation in the evolving plasma after the reflection from the liquid target surface. For accurate modeling of the above-described processes, we used available data of the experimental optical properties for laser reflection from liquid tin;[16,17] then, since one of the main features of the collision-induced absorption is a quadratic dependence of the absorption coefficient on the density with a weak dependence on the temperature,[18] laser photons absorption in vapor was simulated with this approach and the inverse bremsstrahlung absorption was used for simulation of laser photons interaction with plasma. In our Monte Carlo modeling of laser photons absorption, reflection, and re-absorption in liquid/vapor/plasma as well as photon transport in plasma interplays with surface vaporization process. The upgraded HEIGHTS package includes model for tin target vaporization based on the kinetics of evaporation. The model establishes the connection between the surface temperature and the net atom flux leaving the surface taking into account the possibility of recondensation.[19] Vaporized layer above the target surface initializes process of laser photons absorption in vapor/plasma that prevents their penetration to the target surface. At the same time, radiated plasma photons add their energy to the heating of droplet and this energy load to the target can be significant from the well-developed hot plasma plume.

III. VARIOUS PROCESSES AFFECTING EUV PRODUCTION

A. Laser energy absorption in plasmas from tin foil and tin droplet

We studied and benchmarked in our previous work[10,11] the effect of laser beam parameters on EUV radiation in plasma created from a tin foil. We investigated the wavelength effects of the laser light on the temporal and spatial features of EUV radiation emission and obtained approximately the same conversion efficiency (CE) from plasmas created by CO_2 and Nd:YAG lasers with optimized parameters for both lasers. This situation is different when small droplets are used as the target for plasma creation. Efficiency of such systems for EUV radiation is significantly lower than efficiency of devices using planar targets. While the decrease in CE for Nd:YAG laser is explained mainly by the necessity to use reasonable small spot size in correspondence with droplet diameter, the decrease of CO_2 laser efficiency is, however, also influenced by lower vaporization rate that results in small plasma/vapor plume developed by this laser from the small droplet.

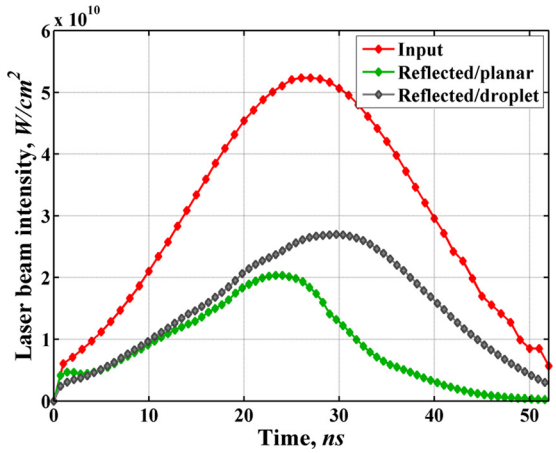

FIG. 1. Incident and reflected laser energy in plasmas created from tin planar and droplet targets with 30 μm spot size.

One of the main important processes during target/plasma evolution in LPP systems is the rate of laser energy absorption and reflection during the course of laser pulse deposition. Figure 1 illustrates the difference in the absorption of CO_2 laser (10.6 μm wavelength) during the development of plasma plumes created from a planar target and from a droplet with the same laser beam parameters, i.e., in this case 30 μm spot, 5×10^{10} W/cm^2 intensity and laser pulse width 30 ns (FWHM). Less energy is absorbed in droplet target configurations due to the plasma geometrical evolution and motion around the droplet.

In our simulations as well as in experiments,[20] the CE of source from 30 μm droplet heated by CO_2 laser is very low, around 0.5%. The CE for planar target with the same laser beam parameters is 1%. Figure 2 shows comparison of percentage of the absorbed energy for these conditions and also, in comparison with the energy absorption of laser beam with larger spot size, which gives higher CE of EUV of about 2.15% in our HEIGHTS simulations compared well to 2.3% in recent experiments of similar conditions.[21] The processes of intense absorption of laser photons in plasma were delayed in the case of larger laser spot (Fig. 2) due to almost 10 times lower laser intensity. The lower intensity delayed the process of vapor/plasma plume formation, suitable for CO_2

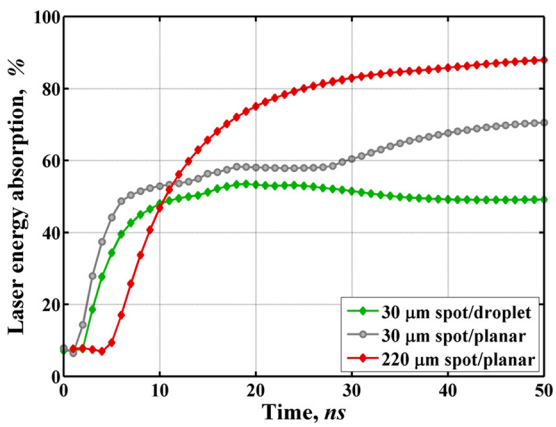

FIG. 2. Comparison of absorbed laser energy in plasmas created from tin planar and droplet targets using laser with small spot size and from planar with large laser spot size.

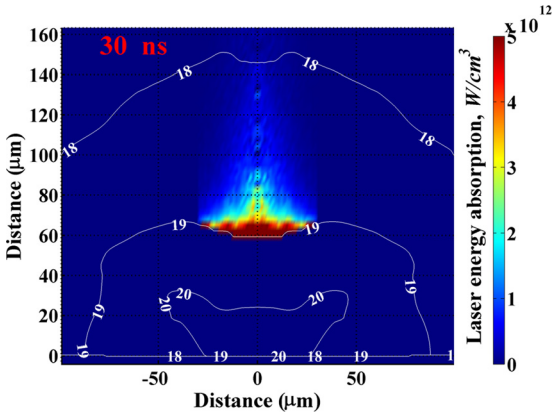

FIG. 3. Laser energy absorption at 30 ns in plasma created from tin foil by CO_2 laser. Plasma density is shown by white contours.

laser photons absorption. We used 5×10^{10} W/cm^2 and 6.5×10^{9} W/cm^2 intensities for the small and large spot sizes, respectively, since these produce most efficient plasma for EUV source with approximately the same range of plasma temperatures, i.e., up to 55 eV.

With similar initial reflection rate in both planar and spherical target cases, during laser beam heating solid targets, the subsequent absorption in the developed plasma plume is almost two times less in the case of spherical target.

Spatial distribution of the absorbed laser energy at this time (Figs. 3 and 4) shows that planar target provides larger area in the direction of laser beam suitable for CO_2 photons absorption. One of the main reasons for this behavior is higher, more than five times, vaporization rate from the planar target due to plasma and geometrical effects. The differences in vaporization process and hydrodynamic evolution of plasma plumes from planar and spherical targets determined the difference in location and shape of area for the laser photons absorption and, as consequence, the location and intensity of EUV emission area. Figures 5 and 6 show spatial distribution of plasma temperature and density from planar and droplet targets, respectively, with approximately similar maximum temperature values. However, plasma from the planar target has larger area with better parameters for EUV photons emission, such as 30–40 eV temperature and 10^{19}–10^{20} cm^{-3} electron density.

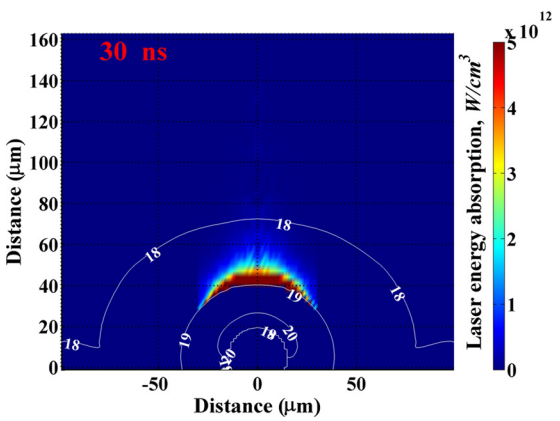

FIG. 4. Laser energy absorption at 30 ns in plasma created from tin droplet by CO_2 laser. Plasma density is shown by white contours.

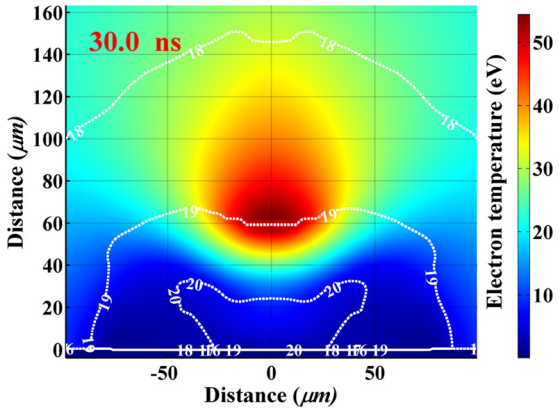

FIG. 5. Temperature and density (white contours) distribution at 30 ns in plasma created from tin foil by CO_2 laser.

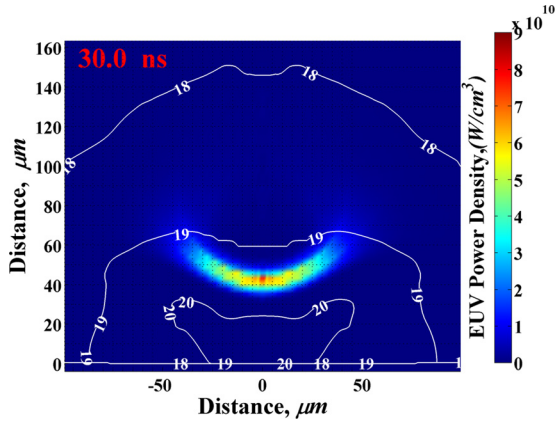

FIG. 7. Location and intensity of the EUV source at 30 ns from the planar target.

The implemented models in HEIGHTS Monte Carlo description for the radiation transport include detailed calculation of the opacities that allow precise prediction of EUV source location and strength based on the fundamental description of plasma radiation processes. The models were widely benchmarked against CMUXE experimental results[10] and other extensive experimental studies, e.g., by Spitzer *et al.*,[22] for various laser beam parameters. Figures 7 and 8 show EUV source location and intensity in plasma created by CO_2 laser from planar and spherical targets, respectively. Planar target produces EUV radiation source with lower intensity, because of the higher reabsorption in upper plasma layers resulting in high temperature values. However, the source has larger EUV volume explained by the larger area with overall conditions appropriate for the better EUV radiation emission.

B. Influence of laser energy and wavelength on vaporization rate

Mass-limited targets such as small tin droplets are considered among the best choices for cleaner operation and longer lifetime of the optical system because of the lower mass of atomic debris produced by the laser beam that could reach the optical mirror collection system. Recently, we simulated and optimized laser beam parameters to produce efficient EUV source from 100 μm and 30 μm tin droplets.[12,23] Modeling results as well as experimental data[6] showed the importance of pre-pulse laser parameters for the target vaporization and creation of initial matter for the main laser pulse.

The dependence of vaporization rate on laser beam wavelength, energy, and spot size has nonlinear tendency since this process, in self-consistent simulation, depends on (1) the time of initiation of laser energy absorption in plasma that reduces energy load to the target; (2) geometry of target, since heating of droplet by the laser and by the plasma itself can cause vaporization from the sides of droplet; and (3) generated photon flux in evolving plasma and transport to original target surface. Figures 9 and 10 show vaporization rate during the heating of 20 μm droplet by the laser beam with 1064 nm wavelength and different intensities. Tin droplet with such size has mass of 3×10^{-8} g. Laser beam with 10^{12} W cm^{-2} intensity only vaporized about half of the droplet utilizing relatively large part of energy (30 mJ) for creation of pre-plasma that can significantly decrease the efficiency of the whole dual-beam system. The high absorption of 1064 nm in the developed plasma plume, as well as the reflection from solid/liquid tin are the reasons of the smaller vaporized mass.

In the case of small mass-limited droplets analyzed in our study, maximum droplet mass ablation is the most important criteria for an efficient EUV source. The evaporated mass and the size of prepared plasma evolution in this case

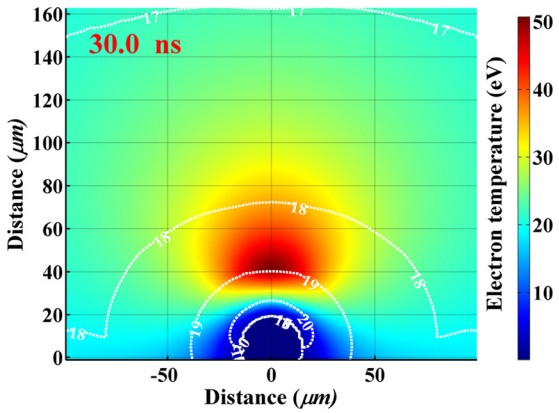

FIG. 6. Temperature and density (white contours) distribution at 30 ns in plasma created from tin droplet by CO_2 laser.

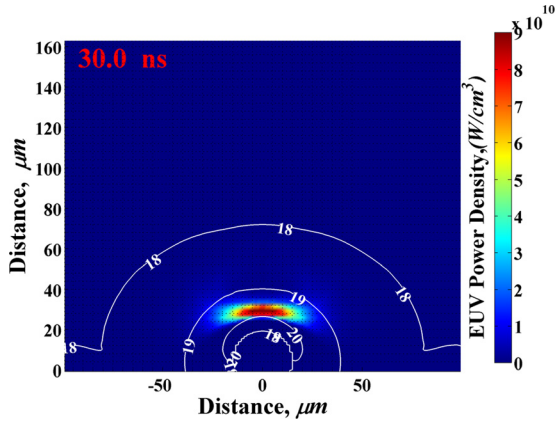

FIG. 8. Location and intensity of the EUV source at 30 ns from the droplet target.

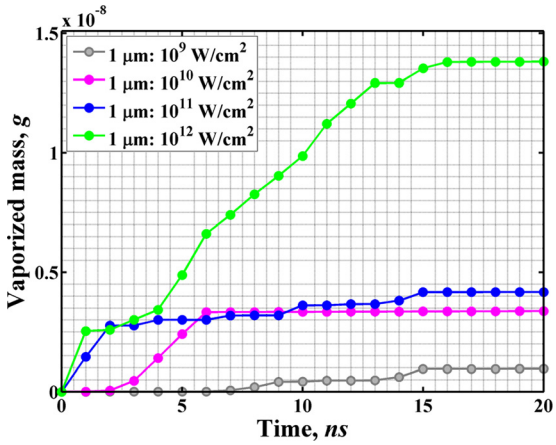

FIG. 9. Dependence of evaporation dynamics on pre-pulse laser beam intensity at 1064 nm wavelength: total evaporated mass in g.

strongly depend on laser parameters, i.e., wavelength and intensity.

The 1064 nm pre-pulse laser cannot efficiently evaporate the entire droplet due to the relatively low critical density. Laser with this wavelength can be used, e.g., to split the droplet onto small fragments, then fragments are distributed and heated by the main laser, as it was illustrated in recent experiments.[24] However, efficient splitting of droplets was only achieved at higher pre-pulse laser intensities[24] that results in producing energetic tin ions even at the pre-pulse stage that could affect the lifetime of optical collecting system. In case of lower intensities of 1064 nm laser,[25] lower evaporation rate of droplet will result in high accumulation of tin cluster debris in the chamber.

The fourth harmonic of Nd:YAG laser has a higher critical density and can be better solution for higher evaporation of the small droplets with minimum energy loss. In such case, most of the 20 μm droplet is vaporized when we used laser beam with 266 nm wavelength and 0.65 mJ energy as shown in Fig. 10. This is also significant in reducing contamination from macroscopic debris and potential increase in components lifetime.

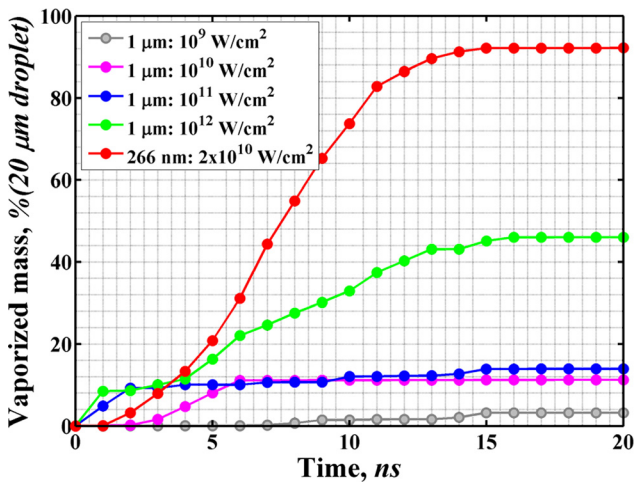

FIG. 10. Percentage of evaporated mass from 20 μm droplet. Laser beam parameters used are 20 μm spot size and 10 ns duration.

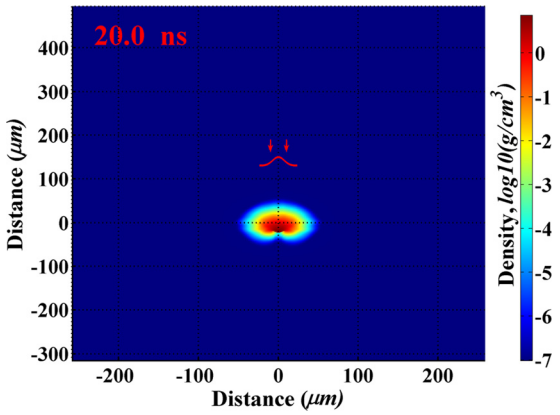

FIG. 11. Mass density distribution after pre-pulse (10 ns FWHM). Pre-plasma was created by laser beam with 266 nm wavelength and intensity of 2×10^{10} W/cm^2.

The advantages of pre-heating small tin droplets by laser with shorter 266 nm wavelength are, therefore, higher vaporization rate and lower temperatures of the developed plasma plume. The higher vaporization rate allows almost complete droplet vaporization and the lower temperatures of plasma plume reduce the fluence and energy of ions debris. This suggested approach could be further used to significantly extend the optical collection system lifetime.

C. Dependence of CE on density evolution of micro-droplets

We also studied in our simulations the use of smaller droplets with diameter up to 10 μm to predict the minimum size of droplet that is sufficient for production of the efficient EUV source with minimum debris creation.

It is known from experiments with tin planar target that devices with CO_2 laser allow source operation using longer pulses (100 ns and more) without significant reduction in the efficiency of EUV output.[26] This can be explained by the lower mass ablation rate from the CO_2 laser beams with the longer wavelength and comparatively low value of the critical density for absorption of these photons. We obtained the same tendency in our modeling results for planar targets. However, simulations with the CO_2 heating of plasma/vapor mix, created from 20 μm droplet (Fig. 11) and expanded during 100–500 ns, show dependence of the CE on pulse

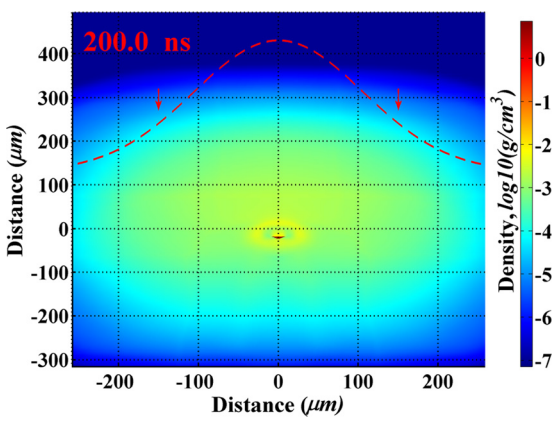

FIG. 12. Mass density distribution after 200 ns delay.

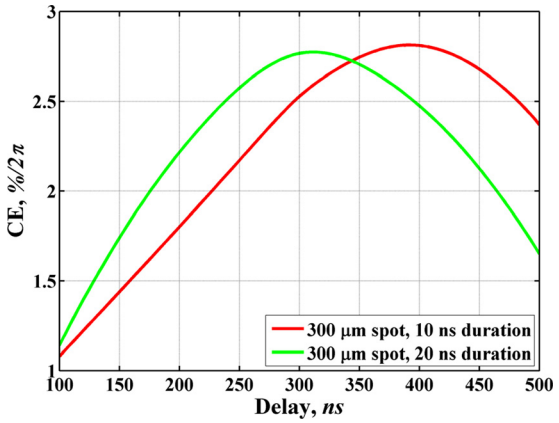

FIG. 13. CE from 20 μm droplet as function of delay time between the prepulse and the main CO_2 laser pulse.

duration. The expanded plume mixture during these times has relatively low mass density with almost uniform distribution (Fig. 12).

We predicted the optimum duration of CO_2 laser beam, such as 10 or 20 ns pulse width (FWHM), to have maximum CE of about 2.8% from a target with 20 μm diameter as shown in Fig. 13. The further increase in pulse width to 30 ns resulted in a decrease of maximum CE to about 2% due to low mass density for development of efficient photons source during the entire course of laser energy deposition.

Further analyses of the dependence of EUV output on the prepulse density mixture showed that plasma created from 10 μm droplet or smaller may not be an efficient source. The maximum obtained CE was about 1.3% with optimized pulse duration of 10 ns and spot size of 200 μm. This value is consistent with recent experimental result.[20]

IV. CONCLUSION

We optimized several parameters using dual-beam lasers to predict the minimum size of droplets sufficient for production of an efficient EUV source with minimum debris creation. Such detailed simulations were possible with our comprehensive and advanced models for the description of plasma physics processes included in our HEIGHTS simulation package. HEIGHTS package is a fully 3D that integrate all phases of beam target interactions for laser and discharge plasma devices and the subsequent evolution of target debris and plasma expansion.

We predict that the fourth harmonic of Nd:YAG laser is the best choice for pre-plasma creation from small droplets. The pre-plasma evolved from a droplet with 20 μm diameter can be an efficient target for subsequent heating using a main CO_2 laser to produce EUV source with up to 2.8% conversion efficiency. The most efficient EUV source for the next generation lithography will depend on many target and driver parameters and can be studied efficiently using advanced computer simulations to accelerate source development and enhance system lifetime, with significant cost saving of designing and running extensive experiments.

ACKNOWLEDGMENTS

This work is partially supported by the College of Engineering, Purdue University. We gratefully acknowledge the computing resources provided by the Fusion cluster operated by the Laboratory Computing Resource Center at Argonne National Laboratory.

[1]A. Hassanein *et al.*, in *EUV Sources for Lithography*, edited by V. Bakshi (SPIE, Bellingham, Washington, USA, 2006), Chap. 9, pp. 277–298.
[2]U. Stamm *et al.*, Proc. SPIE **5037**, 119 (2003).
[3]T. Higashiguchi, Appl. Phys. Lett. **88**, 161502 (2006).
[4]J. R. Hoffman *et al.*, Proc. SPIE **5751**, 892 (2005).
[5]G. Schriever *et al.*, J. Micro/Nanolith. MEMS MOEMS **11**, 021104 (2012).
[6]J. Fujimoto *et al.*, Proc. SPIE **8322**, 83220F (2012).
[7]V. Sizyuk, A. Hassanein, and T. Sizyuk, J. Appl. Phys. **100**, 103106 (2006).
[8]V. Sizyuk, A. Hassanein, and V. Bakshi, J. Micro/Nanolith. MEMS MOEMS **6**, 043003 (2007).
[9]V. Sizyuk, A. Hassanein, and T. Sizyuk, Laser Part. Beams **25**, 143–154 (2007).
[10]A. Hassanein, V. Sizyuk, T. Sizyuk, and S. S. Harilal, J. Micro/Nanolith. MEMS MOEMS **8**(4), 041503 (2009).
[11]A. Hassanein, V. Sizyuk, S. S. Harilal, and T. Sizyuk, Proc. SPIE **7636**, 76360A (2010).
[12]A. Hassanein, T. Sizyuk, V. Sizyuk, and S. S. Harilal, J. Micro/Nanolith. MEMS MOEMS **10**, 033002 (2011).
[13]A. Hassanein, Fusion Eng. Des. **60**, 527–546 (2002).
[14]A. Hassanein *et al.*, Fusion Eng. Des. **69**, 781–787 (2003).
[15]V. Sizyuk and A. Hassanein, Nucl. Fusion **50**, 115004 (2010).
[16]J. P. Petrakian, A. R. Cathers, J. E. Parks, R. A. MacRae, T. A. Callcott, and E. T. Arakawa, Phys. Rev. B **21**, 3043–3046 (1980).
[17]G. Cisneros, J. S. Helman, and C. N. J. Wagner, Phys. Rev. B **25**, 4248–4251 (1982).
[18]G. G. Grigoryan, A. G. Leonov, E. A. Manykin, A. A. Rudenko, M. G. Sitnikov, and A. N. Starostin, J. Exp. Theor. Phys. **97**, 678–687 (2003).
[19]A. Hassanein, G. L. Kulcinski, and W. G. Wolfer, Nucl. Eng. Des.-Fusion **1**, 307–324 (1984).
[20]H. Mizoguchi *et al.*, Proc. SPIE **7969**, 796908 (2011).
[21]J. R. Freeman, S. S. Harilal, T. Sizyuk, A. Hassanein, and B. Rice, Proc. SPIE **8322**, 83220H (2012).
[22]R. C. Spitzer *et al.*, J. Appl. Phys. **79**, 2251 (1996).
[23]T. Sizyuk and A. Hassanein, Proc. SPIE **8322**, 2K (2012).
[24]S. Fujioka, M. Shimomura, Y. Shimada, S. Maeda, H. Sakaguchi, Y. Nakai, T. Aota, H. Nishimura, N. Ozaki, A. Sunahara, K. Nishihara, N. Miyanaga, Y. Izawa, and K. Mima, Appl. Phys. Lett. **92**, 241502 (2008).
[25]K. Nishihara, A. Sunahara, A. Sasaki, M. Nunami, H. Tanuma, S. Fujioka, Y. Shimada, K. Fujima, H. Furukawa, T. Kato, F. Koike, R. More, M. Murakami, T. Nishikawa, V. Zhakhovskii, K. Gamata, A. Takata, H. Ueda, H. Nishimura, Y. Izawa, N. Miyanaga, and K. Mima, Phys. Plasmas **15**, 056708 (2008).
[26]Y. Tao *et al.*, Appl. Phys. Lett. **92**, 251501 (2008).